Available online at www.sciencedirect.com

ScienceDirect

Proceedings of the Combustion Institute 36 (2017) 1523–1530

Proceedings of the Combustion Institute

www.elsevier.com/locate/proci

Binary diffusion coefficients and non-premixed flames extinction of long-chain alkanes

Changran Liu [a], Runhua Zhao [b], Rui Xu [a], Fokion N. Egolfopoulos [b], Hai Wang [a,*]

[a] *Mechanical Engineering Department, Stanford University, Stanford, CA 94305-3032, USA*
[b] *Aerospace and Mechanical Engineering, University of Southern California, CA 90089-1453, USA*

Received 4 December 2015; accepted 8 July 2016
Available online 19 July 2016

Abstract

The current study aims to resolve the experimental and modeling discrepancies previously observed for the extinction strain rates of counterflow, non-premixed *n*-decane and *n*-dodecane/nitrogen mixture versus oxygen. To achieve this goal, a recently developed transport theory of cylindrical molecular structure in dilute gases is used to model the binary diffusion coefficients of long-chain *n*-alkanes up to *n*-dodecane in N_2 and He. The updated diffusion coefficients are found to be significantly different from early estimates made from the law of corresponding states. The diffusion coefficient update removes the early difficulties in modeling the extinction strain rates for non-premixed extinction of *n*-decane and *n*-dodecane. It was found that the mixture averaged transport formulation can provide good predictions provided that the Soret effect on the transport of large fuel molecules is properly accounted for.

Keywords: Diffusion coefficients; Reaction kinetics; Alkanes; Flame extinction

Introduction

Flame properties involving diffusion-kinetic coupling are critical to a basic understanding of combustion properties of hydrocarbon fuels [1]. The extinction state of laminar, non-premixed counterflow flames represents one such key property. A large number of studies have been conducted to date especially in light of the recent interest in the combustion kinetics of real fuels and their single or multi-component surrogates (see, e.g., [2–11]). Holley et al. [8] carried out a sensitivity analysis of non-premixed extinction strain rate with respect to kinetic and transport model parameters. It was found that the flame extinction responses could be particularly sensitive to the mass diffusivity of the fuel, especially for heavy fuel molecules. The cause is quite clear, as in these flames fuel diffusion is typically slow due to the fuel size and weight but diffusion is critical to supplying the fuel to the thermal mixing layer, allowing it react with the oxidizer flowing from the opposite direction. Won et al. [3] developed a radical index method for determining the chemical kinetic

* Corresponding author. Fax: +1 650 723 1748.
E-mail address: haiwang@stanford.edu (H. Wang).

http://dx.doi.org/10.1016/j.proci.2016.07.036
1540-7489

contribution to non-premixed flame extinction of large hydrocarbons. They showed the mass diffusivity of the fuel plays a role critical to the flame extinction; and it becomes possible to isolate the fuel kinetic effects only when the transport effects are properly accounted for.

A class of compounds of particular interest to real liquid fuels is normal paraffin. Previously, Ji et al. [10] measured the extinction strain rates, K_{ext}, of counterflow, non-premixed *n*-decane (*n*-$C_{10}H_{22}$) and *n*-dodecane (*n*-$C_{12}H_{26}$) flames. They found that JetSurF 1.0 [12] overpredicts the K_{ext} data notably. Interestingly, the model predicts the laminar flame speeds and shock tube ignition delay time rather well. Sensitivity analyses suggest that the uncertainty in the kinetic parameters alone could not explain the observed discrepancies between the experimental and computed K_{ext}. Rather, sensitivity tests suggested that the uncertainties of the transport properties could be the cause for the discrepancy.

In the JetSurF effort [12], the diffusion coefficients of long-chain *n*-alkanes were calculated via the Lennard-Jones (LJ) 12-6 potential parameters for the self-interaction of the hydrocarbon molecules. These potential parameters were only rough estimates as they are based on the equations of the law of corresponding states [13] and the use of basic phase-change properties including the critical pressure and temperature and boiling points. The method was used earlier for estimating the potential parameters of polycyclic aromatic hydrocarbons [14]. Since the method is empirical and its use for large *n*-alkanes represents an extrapolation from which the equations were developed, the potential parameters can be inaccurate obviously. Additional uncertainties may include the use of the empirical mixing rule and the fact that there is no obvious reason why spherical, isotropic potential interactions are adequate for chain-like *n*-alkane molecules. Jasper and coworkers [15, 16] carried out classical trajectory studies of several *n*-alkanes in some typical diluent gases to determine diffusion collision cross sections. They showed that indeed diffusion coefficients of *n*-alkanes estimated from the use of the law of corresponding states deviate quite notably from the classical trajectory results. Their work examined *n*-alkane molecules up to *n*-heptane.

There are two principal objectives here. First, we extend a recently developed transport theory of cylindrical molecular structure in dilute gases [17] to model the binary diffusion coefficients of long-chain *n*-alkanes up to *n*-dodecane in N_2 and He. This is a generalized theory based on a gas kinetic theory analysis of the interaction of a point mass with a carbon nanotube-like structure using axial symmetric anisotropic potential function. The diffusion coefficient model is verified against experimental data collected by McGivern and Manion [18,19]. Next, we show that the non-premixed flame K_{ext} of *n*-$C_{10}H_{22}$ and *n*-$C_{12}H_{26}$ of Ji et al. [10] can be predicted accurately with the updated diffusion coefficients with either the multicomponent or mixture averaged transport formulation, provided that the Soret effect on the transport of large fuel molecules is accounted for.

Theory and model of diffusion coefficients

The binary diffusion coefficients are customarily calculated from [20]

$$D_{12} = \frac{3}{8}\sqrt{\frac{k_B T}{2\pi m_r}}\frac{1}{N\sigma_{12}^2\Omega^{(1,1)^*}(T^*)}, \tag{1}$$

where k_B is the Boltzmann constant, T is the temperature, m_r is the reduced mass, N is the number density of the gas, σ_{12} is the collision diameter and $\Omega^{(1,1)^*}(T^*)$ is the reduced collision integral, T^* is the reduced temperature, i.e., $T^* = k_B T/\varepsilon_{12}$, and ε_{12} is the well depth. Equation (1) is the first-order term of the Chapman–Enskog (CE) expansion employing the Lennard-Jones (LJ) 12-6 potential function. In general, the LJ 12-6 potential parameters are approximated by the following mixing rule:

$$\sigma_{12} = \frac{\sigma_1 + \sigma_2}{2}, \tag{2}$$

$$\varepsilon_{12} = \sqrt{\varepsilon_1 \varepsilon_2}. \tag{3}$$

For long-chain alkanes, the binary diffusion coefficient calculated from Eqs. (1)–(3) can have at least two problems. First, there is little to no fundamental basis for a long-chain molecule to assume an isotropic potential of interaction regardless what type of molecules it interacts with. Second, there is no reason why the mixing rule should be appropriate when we use the self-collision potential parameters that are derived from single-component viscosity or other data, yet this is usually the method by which the self-collision parameters are derived [21]. Indeed, for small spherical-like molecule like methane, Eq. (1) gives good prediction (see, e.g., [22]). Recent molecular dynamics (MD) simulations by Chae et al. [23] however suggest that Eq. (1) can deviate from the MD results by as much as 20%.

Recently, a generalized transport theory was developed for nanosized cylindrical structures (e.g., nanotubes) in the low-pressure and dilute limit considering the potential function of interactions between a cylinder and bath gas [17]. In this theory, the drag force due to relative motion of a small cylinder in a dilute gas and in the free molecule regime (cylinder diameter $\ll$ length $\ll$ mean free path of the gas) was obtained analytically from a rigorous gas-kinetic theory analysis. The expression for the binary diffusion coefficient may be derived from the Einstein–Smoluchowski relation via the drag coefficient k_d. That is, $D = k_B T/k_d$ [24]. The

approach yields result identical to Eq. (1) in the limit of isotropic potential function [25, 26].

The generalized theory gives the binary diffusion coefficient for n-alkane in a diluent gas M as [27]

$$D_{a,M} = \left[\frac{8}{3\pi} \sqrt{\frac{2m_r}{\pi k_B T}} N(n_C - 1) Q(\Phi, T) + \frac{1}{D_{CH_4,M}} \right]^{-1}, \quad (4)$$

where the subscript "a" represents the n-alkane molecule, n_C is the number of carbon atom in the n-alkane molecule, and $Q(\Phi, T)$ is the collision cross section, Φ is the potential function, and $D_{CH_4,M}$ is the binary diffusion coefficient of CH_4 in M to account for the edge effect. The values of $D_{CH_4,M}$ (M = N_2 and He) were taken from a recent experimental study [18].

The cross section $Q(\Phi, T)$ is a quintuple integral over the Boltzmann energy distribution and four geometric parameters (two lengths and two angles) due to interaction of a small gas molecule with a cylinder of finite length and radius. The value of Q was obtained numerically as a function of the potential parameters and temperature. Our approach differs from that of Jasper and Miller [16] at the theoretical level. While Jasper and Miller fitted the classical trajectory results to an effective isotropic potential for diffusion coefficient evaluation, we determine the collision cross section Q analytically from an anisotropic potential function and collision dynamics. The advantage of the Jasper–Miller method is that it relies on interaction potentials from electronic structure calculation; whereas the advantage of our approach is that it yields gas-kinetic expression to account for the anisotropic interactions directly.

In the limit where an axial symmetric intermolecular potential function may be employed (i.e., neglecting edge effects and the zigzag nature of the n-alkane molecule), we approximate the potential function as [27]

$$\Phi(r^*) = 8\varepsilon_{-CH2-,M} \frac{\sigma_{-CH2-,M}}{l_{C-C}} \times [C_6(r^* - \gamma^*)^{-11} - C_3(r^* - \gamma^*)^{-5}], \quad (5)$$

where r^* is the reduced distance $r^* = r/\sigma_{-CH2-,M}$, r is the distance of M to the center axis of an n-alkane molecule taken here to be a cylindrical structure, $\varepsilon_{-CH2-,M}$ and $\sigma_{-CH2-,M}$ are the well depth and collision diameter in an effective LJ 12-6 potential function for the interaction of M with a unit length of the n-alkane molecule, which may be represented by the methylene group –CH_2–, γ^* is a dimensionless length factor given by $\gamma/\sigma_{-CH2-,M}$, which accounts for the finite radius of the cylindrical structure, $2 \times l_{C-C}$ (cos(109.47°) × 1.54 (Å) = 2.514 Å) is the distance of two adjacent C atoms along the center axis of the cylinder, and C_6 and C_3 are parameters that may be evaluated by summing the contribution of the methylene groups ($C_6 = 0.7728$ and $C_3 = 1.178$). From geometric considerations it may be shown that $\gamma = 0.12$ Å for n-alkane molecules. Like the application of the conventional LJ 12-6 potential function to molecular transport, we have two potential parameters, $\varepsilon_{-CH2-,M}$ and $\sigma_{-CH2-,M}$ that are treated as the geometric and arithmetic averages of the self-interaction potential parameters (i.e., Eqs. (2) and (3)). The values of the self-interaction potential parameters used here are: $\sigma_{N_2} = 3.652$ Å, $\varepsilon_{N_2}/k_B = 98.4$ K [28], and $\sigma_{He} = 2.639$ Å, $\varepsilon_{He}/k_B = 10.8$ K [22]. The pseudo "self-collision" well depth and collision diameter of the –CH_2– group are fitted into relevant experimental data, as will be discussed later.

Measurement of extinction strain rate

To supplement the data from a previous study [10], we made additional measurements for non-premixed flame extinction of n-dodecane. The experiments were carried out at atmospheric pressure in the counterflow configuration (see, [9,29–31]). Details of the measurement have been discussed elsewhere [10]. Briefly, non-premixed flames were established by impinging a fuel/N_2 stream on to an opposing ambient temperature O_2 stream. The burner nozzle diameter and the burner separation distance were 1.4 cm. Screens were placed in the burner to assure top-hat burner velocity profile at the nozzle exit. The gaseous flow rates were metered using sonic nozzles, which were calibrated using a dry-test meter with a reported accuracy of ± 0.21%. The upstream pressure of each sonic nozzle was monitored by a pressure gauge with ± 0.25% precision. The vaporization system included a precision syringe pump of ± 0.35% accuracy and a glass nebulizer (Meinhard TR-50-A1), through which the liquid fuel was injected as fine droplets into a crossflow of heated nitrogen. All gas lines were heated to prevent fuel vapor condensation. The temperature of the gas lines was measured with K-type inline thermocouples. The temperature of the unburned fuel/N_2 stream, T_u, was measured at the center of the burner exit. The variation of this temperature is within ± 5 K. Flow composition uncertainty has been determined to be less than 0.5% [10]. Flow velocity measurements were made by seeding the flow with submicron size silicon oil droplets and by using particle image velocimetry (PIV). The uncertainty associated with the PIV measurements is within 0.8–1.0% [10]. The maximum absolute axial velocity gradient on the fuel side of the hydrodynamic zone was defined as the strain rate, K, and K_{ext} was determined for a near extinction flame. The uncertainty of K_{ext} to be

Table 1
Summary of computational cases.

Case	Source of parameters	Formulation	Soret effect
I	JetSurF [12][a]	Multicomponent	Yes
II	JetSurF [12][a]	Multicomponent	No
III	This work	Mixture averaged	Yes[b]
IV	This work	Multicomponent	Yes

[a] Estimated using the law of corresponding state [13,14].
[b] Using the thermal diffusion ratio of Rosner et al. (Eq. (6)) [39].

quoted here is the $\pm 2\sigma$ standard deviation of repeated measurements.

Numerical simulation of flames

K_{ext} was computed using an opposed-jet flow code [32] developed originally by Kee et al. [33]. This code was modified to allow the use of a wider range of boundary conditions than the initial version and to account for thermal radiation of CH_4, H_2O, CO and CO_2 at the optically thin limit [34]. The JetSurF 1.0 kinetic model [12] was used to describe the high-temperature pyrolysis and oxidation of n-$C_{10}H_{22}$ and n-$C_{12}H_{26}$.

For K_{ext} computations, a two-point continuation approach solves for K at the state of extinction [35,36]. The experimental values of the axial velocity gradients at the burner exits were considered as the respective boundary conditions in the simulation [31]. The code was integrated with the Sandia Transport subroutine libraries [37] with the diffusion coefficients of H and H_2 in several key diluent gases updated from Ref. [38] and those of n-$C_{10}H_{22}$ and n-$C_{12}H_{26}$ in N_2 from the current diffusion coefficient model. Molecular transport was treated comparing both mixture-averaged formulation and multicomponent formulation.

We note that the mixture-averaged transport formulation of the original Sandia PREMIX and OPPDIF codes does not consider the Soret effect of large/heavy molecules even if the thermal diffusion (TDIF) keyword is turned on. To account for thermal diffusion of heavy fuel molecules, the approximation of Rosner et al. [39] for the thermal diffusion factor α_T was implemented into the mixture-averaged formulation. The thermal diffusion factor of species B in A takes the form of

$$\alpha_T = [0.454d(\Lambda + 0.261) + 0.116(\Lambda - 1)] \times [1 - C/T], \quad (6)$$

where Λ is related to molecular size disparity, which may be evaluated by $\Lambda \cong 1.31\mathrm{Sc}(1+d)^{-1/2}$, Sc is the Schmidt number, $d = (M_B - M_A)/M_B + M_A$ is the normalized molecular mass disparity, and

$$C = 1.45[\varepsilon_{BA}/k_B - 85]. \quad (7)$$

For the cases considered here, $C/T << 1$ and thus the temperature correction is unimportant. Four computational cases were used to examine the impact of updated binary diffusion coefficients on non-premixed flame extinction of n-$C_{10}H_{22}$ and n-$C_{12}H_{26}$. They are summarized in Table 1. While Cases I and II test the predictions of K_{ext} using the old diffusion coefficient estimates [12] from the law of corresponding state with the purpose of comparing the impact of the Soret effect, Cases III and IV test the updated diffusion coefficients.

Results and discussion

Measurements reported by McGivern and Manion [18] for the diffusion coefficients of n-C_4H_{10} in N_2 and He were used as the base data set to fit the two pseudo potential parameters for the self-collision of the –CH_2– group. Also considered are the unpublished data of the same authors for n-C_5H_{12}-N_2, and n-C_5H_{12}, n-C_6H_{14}, and n-C_8H_{18} in He [19]. The temperature range spans from 300 K to 723 K for the available data. The range is narrowed somewhat for large alkanes (e.g., 450 to 700 K for n-C_8H_{18} in He). A fit to all data considered (a total of 29 experimental diffusion coefficient values) with respect to the two pseudo-potential parameters of the –CH_2– group yielded $\varepsilon/k_B = 306$ K and $\sigma = 4.12$ Å. The maximum fitting error is 6 %. It is worthy to note that the accuracy of the low-temperature data of large alkanes may be impacted by their tendencies to stick to the wall of the GC column. Excluding the data of n-C_8H_{18} and n-C_6H_{14} in He at 350 and 400 K, the maximum fitting error is 3.8%, which is comparable to the maximum experimental uncertainty of 3.5%.

Figure 1 shows the comparison of the experimental diffusion coefficients of n-butane in He and N_2 with the current diffusion coefficient model, along with the early estimates from the equation of corresponding state. The agreement is reasonably good for N_2, but the early estimates fail to reproduce the n-butane-He diffusion coefficient. Also shown in the figure are the results of classical trajectory study of Jasper et al. [15] for n-C_4H_{10} in N_2, which are in close agreement of the current results below 1000 K. Although the agreement worsens somewhat towards high temperatures, the difference (3.4% at ~1500 K and 6.3% at ~2000 K) is still too small to impact any flame predictions.

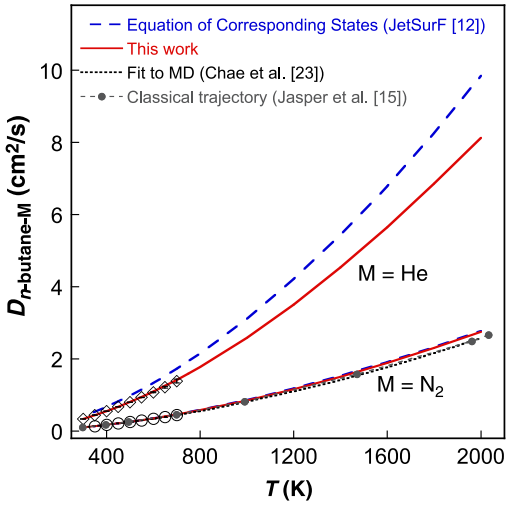

Fig. 1. Binary diffusion coefficients of n-butane-N_2 and n-butane-He at 1 atm pressure. Symbols: experimental data of McGivern and Manion [18]; lines: predictions of various theories, models and estimates (see text).

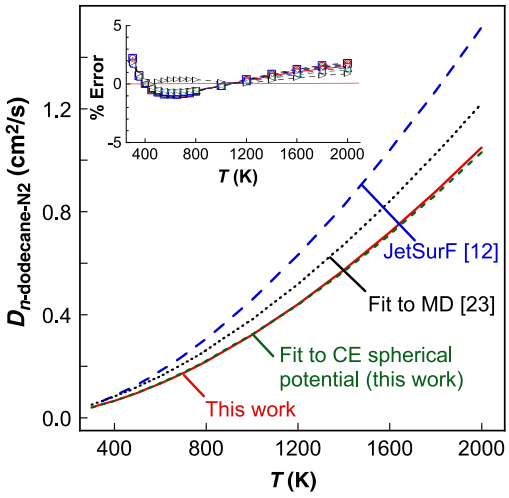

Fig. 2. Binary diffusion coefficient of n-dodecane-N_2 at 1 atm pressure, comparing predictions of various theories and estimates (see text). The inset shows errors from fitting the results of Eq. (4) by Eq. (1) using effective LJ 12-6 potential parameters (values are given in Table 2).

The current diffusion coefficient model yields values for n-$C_{12}H_{26}$ in N_2 substantially smaller than the earlier estimate from the law of corresponding states. As shown in Fig. 2, the current model is as much as 45% lower than the earlier estimate at 1200 K. As will be shown later, this discrepancy is the cause for the overprediction of K_{ext} of n-$C_{10}H_{22}$ and n-$C_{12}H_{26}$ in Ref. [10]. The molecule dynamics simulation of Chae et al. [23] was carried over the temperature range of 500 to 1000 K. They then fitted the MD results to an empirical relation given as $D = AT^B$, where A and B are pairwise parameters. Figure 2 shows that for n-$C_{12}H_{26}$ in N_2, the MD results lie above the current model values, e.g., by about 20% at 1200 K.

Table 2
Effective LJ-12-6 potential parameters of n-alkane-N_2 interactions for calculating the binary diffusion coefficients of n-alkane in N_2.

Species	σ Å))	ε/k_B (K)[a]
n-butane	4.749	101.6
n-pentane	5.086	107.2
n-hexane	5.437	106.8
n-heptane	5.744	111.7
n-octane	6.106	104.2
n-nonane	6.415	103.6
n-decane	6.683	107.8
n-undecane	6.994	103.4
n-dodecane	7.222	109.8

[a] An average value of 106 K may be used for all species considered.

Like Jasper et al. [15], we examined whether the results of our diffusion coefficient model can be fitted into a set of effective LJ 12-6 potential parameters such that Eq. (1) still can be used for flame simulations. Figure 2 shows that indeed the diffusion coefficient can be fitted by these potential parameters over the entire range of temperature considered using the Chapman–Enskog (CE) equation. The potential parameters are specific to each diluent gas, as there is no fundamental basis or practical need to use mixing rules. The inset of Fig. 2 shows that for n-C_4H_{10} to n-$C_{12}H_{26}$ in N_2 the maximum error is below 2% with such fits. Table 2 lists the fitted, effective potential parameter values. Interestingly, while the effective collision diameter is a function of the molecular size, the well depth is not. The small variation of the ε/k_B seen in the table is really just the result of a small degree of error of fitting. We may well use the average value of $\varepsilon/k_B = 106$ K (± 3 K) for all n-alkanes considered.

We shift our focus next to prediction of K_{ext} of n-$C_{10}H_{22}$ and n-$C_{12}H_{26}$ using the effective potential parameters of Table 2. In doing so, we assess the impact of the updated diffusion coefficients on our ability to better predict the experimental data. Figure 3 shows the computed K_{ext} compared to the experimental data collected in the current work from counterflow non-premixed flames of n-$C_{12}H_{26}$ in N_2 at 473 K against O_2 at 300 K over a range of fuel to N_2 mass ratio. Cases I and II both use the diffusion coefficient estimates from the law of corresponding state. These estimates are shown to grossly overpredict K_{ext}. Comparing the Cases I and II, we see that K_{ext} becomes lower with the Soret effect considered. As the fuel is transported to the mixing zone by molecular diffusion, it encounters an upward temperature, which by thermal diffusion pushes it back towards the colder fuel/N_2

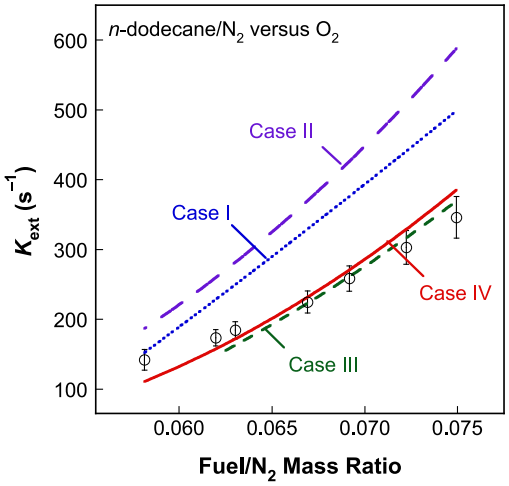

Fig. 3. Extinction strain rate of non-premixed n-$C_{12}H_{26}/N_2$–O_2 flames ($T_u = 473$ K for the fuel jet and 300 K for the oxygen jet) with $p = 1$ atm. Symbols: experimental data (this work); lines are simulations (see Table 1).

jet. Thus, the Soret effect reduces the rate at which the fuel can be transported into the mixing zone and makes the flame more readily to undergo extinction.

The updated diffusion coefficients of n-$C_{12}H_{26}$ in N_2 lead to significantly better predictions for K_{ext} (Cases III and IV), as seen in Fig. 3. As Table 1 shows, there are two differences between the two cases. Case III uses the mixture-averaged transport formula with Rosner's approximate thermal diffusion ratio; Case IV employs multicomponent transport formulation with a more exact thermal diffusion ratio [20]. Interestingly, the computed K_{ext} values do not differ significantly, suggesting that the mixture-averaged formation is adequate at least for the conditions of the present study. Similar comparisons may be made using the K_{ext} data of Ji et al. [10] for both n-$C_{12}H_{26}$ and n-$C_{10}H_{22}$. As Fig. 4 shows the updated diffusion coefficients yield predicted K_{ext} values much closer to the experimental data, whether one uses the mixture-averaged or multicomponent transport. These results indicate that accurate diffusion coefficients of large fuel molecules and the Soret effect are both important elements towards a satisfactory prediction of flame properties that are governed by diffusion-kinetic coupling.

To amplify the above point, we plot in Fig. 5 the structures of the near extinction flames of n-dodecane/N_2 (473 K) versus O_2 (300 K), computed for Case III and IV. Except for the shift in the stagnation surface marked by the vertical dashed-dotted-dashed lines, the two structures are nearly the same. The fuel is transported to the mixing layer by diffusion and is decomposed to a small number

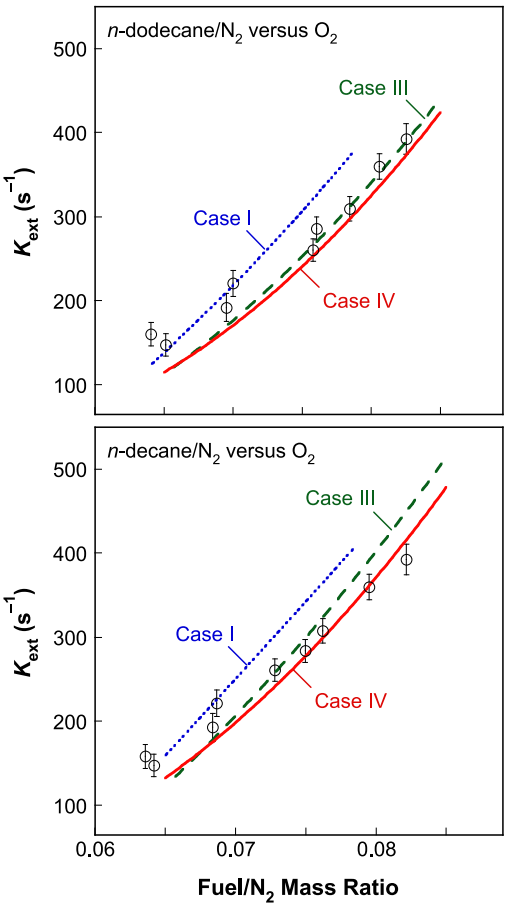

Fig. 4. Extinction strain rate of non-premixed n-$C_{12}H_{26}/N_2$–O_2 flames and n-$C_{10}H_{22}/N_2$–O_2 flames all at $T_u = 403$ K for the fuel jet and 300 K for the oxygen jet, with $p = 1$ atm. Experimental data (symbols) were taken from Ref. [10]; lines are simulations (see Table 1).

of key intermediates, including ethylene, methane, propene, 1,3-butadiene, and hydrogen. The concentrations of these intermediates reach their respective peaks when the concentration of n-$C_{12}H_{26}$ drops to a negligible level. The oxidation of the intermediates follows and the concentrations of the intermediates drop rapidly as they enter into the region where the H atom peaks in its concentration. The molecular diffusion process of the fuel enables the delivery of the fuel into the thermal mixing layer, allowing it to undergo pyrolytic reactions, replacing the fuel by the key intermediates just discussed.

Lastly, we note that the effect of the reduced fuel diffusivity on the flame extinction is clear. A smaller fuel diffusivity (a larger fuel Lewis number) results in a lower peak flame temperature, thus a slower reaction rate in the main reaction zone and a greater tendency of flame extinction. Because of

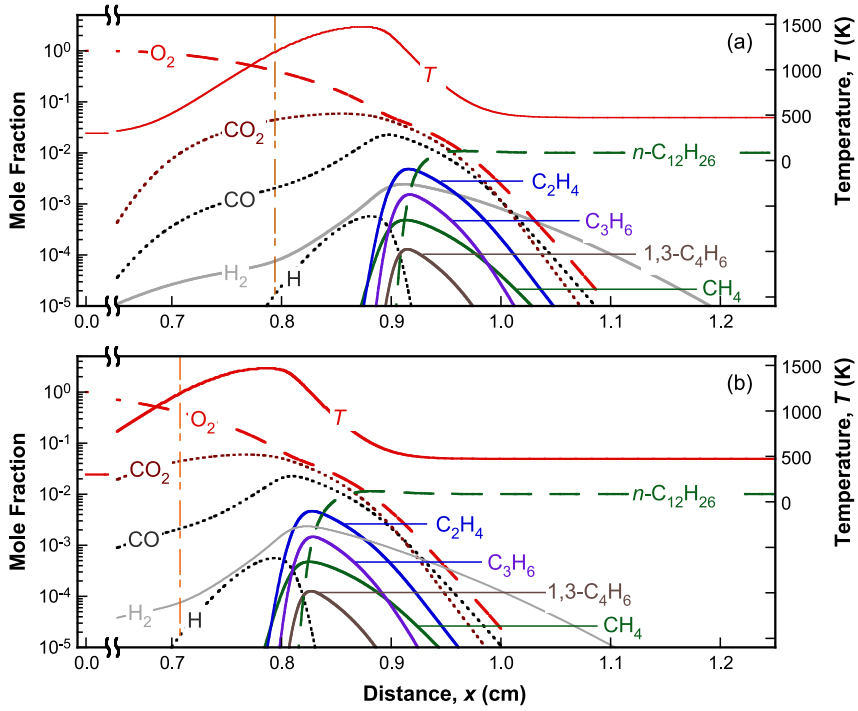

Fig. 5. Structures of *n*-dodecane/N_2 (473 K) versus O_2 (300 K) near extinction flames computed for (a) Case IV (full multicomponent and thermal diffusion transport with updated diffusion coefficients) and (b) Case III (mixture averaged transport with the thermal diffusion ratio of Rosner et al. [39]). The vertical dashed-dotted-dashed line indicates the position of the stagnation surface.

the strong temperature sensitivity of the reaction, small changes to the diffusion coefficient can lead to large changes in the extinction strain rate.

Concluding remarks

The gas-phase binary diffusion coefficient of *n*-alkane in nitrogen is studied using gas-kinetic theory analysis. Effective Lennard-Jones 12-6 potential parameters are proposed for *n*-butane through *n*-dodecane in nitrogen. It is shown that the updated diffusion coefficients resolve the earlier difficulty of predicting the extinction strain rate of non-premixed counterflow flames of *n*-dodecane/N_2 and *n*-decane/N_2 against O_2. The ability of the generalized transport theory for cylindrical structures in dilute gases to reconcile a wide range of binary diffusion coefficient data and to predict the flame extinction data suggests that the theory is valid for the diffusion coefficients of long-chain molecules. It is also shown that the mixture-average transport formulation is adequate for predictions of the extinction strain rate, provided that the Soret effect is taken into consideration.

It is worth to note that the current work dealt with a special class of molecules only, and a generalized transport theory for molecules of arbitrary shapes remain unavailable. From the strong sensitivity we observed for counterflow flame responses with respect the diffusion coefficient of large hydrocarbon species, it is clear that a generalized theory beyond the Chapman–Enskog spherical-potential, elastic treatment is required to offer a thorough description of laminar flame behaviors.

Acknowledgement

The work at Stanford was supported by the Air Force Office of Scientific Research under Grant numbers FA9550-16-1-0051 and FA9550-14-1-0235 and that at USC was supported by the Air Force Office of Scientific Research under Grant no. FA9550-15-1-0409, both under the technical monitoring of Dr. Chiping Li.

References

[1] C.K. Law, *Combustion Physics*, Cambridge University Press, 2006.
[2] M. Colket, T. Edwards, S. Williams, et al., in: 45th AIAA Aerospace Sciences Meeting and Exhibit, 2007, Reno, Nevada, 2007 Paper no. AIAA-2007-0770.

[3] S.H. Won, S. Dooley, F.L. Dryer, Y. Ju, *Combust. Flame* 159 (2012) 541–551.
[4] S. Dooley, S.H. Won, M. Chaos, et al., *Combust. Flame* 157 (2010) 2333–2339.
[5] S.H. Won, W. Sun, Y. Ju, *Combust. Flame* 157 (2010) 411–420.
[6] K. Seshadri, T. Lu, O. Herbinet, et al., *Proc. Combust. Inst.* 32 (2009) 1067–1074.
[7] S. Honnet, K. Seshadri, U. Niemann, N. Peters, *Proc. Combust. Inst.* 32 (2009) 485–492.
[8] A. Holley, X. You, E. Dames, H. Wang, F. Egolfopoulos, *Proc. Combust. Inst.* 32 (2009) 1157–1163.
[9] A. Holley, Y. Dong, M. Andac, F. Egolfopoulos, T. Edwards, *Proc. Combust. Inst.* 31 (2007) 1205–1213.
[10] C. Ji, Y.L. Wang, F.N. Egolfopoulos, *J. Propuls. Power* 27 (2011) 856–863.
[11] B. Li, Y. Zhang, H. Zhang, F.N. Egolfopoulos, *Proc. Combust. Inst.* 35 (2015) 965–972.
[12] B. Sirjean, E. Dames, D. Sheen, et al., A high-temperature chemical kinetic model of n-alkane oxidation. 2009, http://web.stanford.edu/group/haiwanglab/JetSurF/JetSurF1.0/index.html.
[13] L.S. Tee, S. Gotoh, W.E. Stewart, *Ind. Eng. Chem. Fundam.* 5 (1966) 356–363.
[14] H. Wang, M. Frenklach, *Combust. Flame* 96 (1994) 163–170.
[15] A.W. Jasper, E. Kamarchik, J.A. Miller, S.J. Klippenstein, *J. Chem. Phys.* 141 (2014) 124313.
[16] A.W. Jasper, J.A. Miller, *Combust. Flame* 161 (2014) 101–110.
[17] C. Liu, Z.G. Li, H. Wang, *Phys. Rev. E* (2016) (in press).
[18] W.S. McGivern, J.A. Manion, *Combust. Flame* 159 (2012) 3021–3026.
[19] J.A. Manion, W.S. McGivern, *Direct Measurements of Binary Gas Phase Diffusion Coefficients for Combustion Applications*, Argonne National Laboratory, Darien, IL, 2011.
[20] J.O. Hirschfelder, C.F. Curtiss, R.B. Bird, M.G. Mayer, *Molecular Theory of Gases and Liquids*, Wiley, New York, 1954.
[21] R.C. Reid, J.M. Prausnitz, B.E. Poling, *The Properties of Gases and Liquids*, McGraw-Hill, New York, 1987.
[22] R. Trengove, H. Robjohns, P.J. Dunlop, *Ber. Bunsenges. Phys. Chem.* 86 (1982) 951–955.
[23] K. Chae, P. Elvati, A. Violi, *J. Phys. Chem. B* 115 (2010) 500–506.
[24] A. Einstein, *Ann. Phys.* 17 (1905) 549.
[25] Z. Li, H. Wang, *Phys. Rev. E* 68 (2003) 061206.
[26] Z. Li, H. Wang, *Phys. Rev. E* 68 (2003) 061207.
[27] C. Liu, W.S. McGivern, J.A. Manion, H. Wang, *J. Phys. Chem. A* (2016) (submitted).
[28] A. Boushehri, J. Bzowski, J. Kestin, E. Mason, *J. Phys. Chem. Ref. Data* 16 (1987) 445–466.
[29] C. Wu, C. Law, *Symp. Int. Combust.* 20 (1985) 1941–1949.
[30] D. Zhu, F. Egolfopoulos, C. Law, *Symp. Int. Combust.* 22 (1989) 1537–1545.
[31] C. Ji, E. Dames, Y.L. Wang, H. Wang, F.N. Egolfopoulos, *Combust. Flame* 157 (2010) 277–287.
[32] F.N. Egolfopoulos, C.S. Campbell, *J. Fluid Mech.* 318 (1996) 1–29.
[33] R.J. Kee, J.A. Miller, G.H. Evans, G. Dixon-Lewis, *Symp. Int. Combust.* 22 (1989) 1479–1494.
[34] F. Egolfopoulos, *Symp. Int. Combust.* 25 (1994) 1375–1381.
[35] M. Nishioka, C. Law, T. Takeno, *Combust. Flame* 104 (1996) 328–342.
[36] F.N. Egolfopoulos, P.E. Dimotakis, *Symp. Int. Combust.* 27 (1998) 641–648.
[37] R.J. Kee, G. Dixon-Lewis, J. Warnatz, M.E. Coltrin, J.A. Miller, *A Fortran Computer Code Package for the Evaluation of Gas-Phase, Multicomponent Transport Properties*, Sandia National Laboratories, Livermore, CA, 1986.
[38] Y. Dong, A.T. Holley, M.G. Andac, et al., *Combust. Flame* 142 (2005) 374–387.
[39] D. Rosner, R. Israel, B. La Mantia, *Combust. Flame* 123 (2000) 547–560.